



**HAL**  
open science

## Reactive ion beam etching effects on maskless PZT properties

Caroline Soyer, Eric Cattan, Denis Remiens

► **To cite this version:**

Caroline Soyer, Eric Cattan, Denis Remiens. Reactive ion beam etching effects on maskless PZT properties. *Integrated Ferroelectrics*, 2002, 48, pp.221-229. 10.1080/10584580215465 . hal-00149624

**HAL Id: hal-00149624**

**<https://hal.science/hal-00149624v1>**

Submitted on 18 Aug 2022

**HAL** is a multi-disciplinary open access archive for the deposit and dissemination of scientific research documents, whether they are published or not. The documents may come from teaching and research institutions in France or abroad, or from public or private research centers.

L'archive ouverte pluridisciplinaire **HAL**, est destinée au dépôt et à la diffusion de documents scientifiques de niveau recherche, publiés ou non, émanant des établissements d'enseignement et de recherche français ou étrangers, des laboratoires publics ou privés.



Distributed under a Creative Commons Attribution - NonCommercial 4.0 International License

# REACTIVE ION BEAM ETCHING EFFECTS ON MASKLESS PZT PROPERTIES

C. SOYER, E. CATTAN, D. REMIENS

*IEMN / DOAE / MIMM Department  
Université de Valenciennes et du Hainaut-Cambrésis  
Z.I. du de la Petite Savate – 59600 - Maubeuge-France*

**Abstract** : Ion beam etching of sputtered  $\text{Pb}(\text{Zr}_{0.54}\text{Ti}_{0.46})\text{O}_3$  has been performed using pure Ar gas. The etch rate and selectivity ratios between PZT and masks as a function of the process parameters (current density, acceleration voltage, gas pressure) has been investigated.

We have evaluated the PZT surface damage by contact mode AFM. It appears that the roughness increases after ion bombardment, and that the grain boundary zone is preferentially etched.

For some etching parameters, we have also studied electrical damage. Carrying out  $C(V)$  and hysteresis loops  $P(E)$  measurements before and after etching have evidenced these degradation. We have noted a large permittivity decrease after etching process whatever the current density and the acceleration voltage. The ferroelectric damage was illustrated by a large increase of the average coercive field.

**Keywords** : PZT; ion beam etching; etching damage

## I. INTRODUCTION

Ferroelectric thin films have developed a great interest for their applications in microelectromechanical systems (MEMs)  $\text{Pb}(\text{Zr}_{0.54}\text{Ti}_{0.46})\text{O}_3$  (PZT) thin films is one of the most used material because of their interesting piezoelectric properties. Patterning of PZT films has become an essential element of device fabrication. Several techniques have been developed for etching: wet chemical etching [1], ion beam etching (IBE) [2], reactive ion etching (RIE) [3-5], electron cyclotron resonance (ECR) etching [6], and inductively coupled plasma (ICP) etching [7].

The RIE is widely used because it provides, in some etching conditions, high etch rate, high degree of anisotropy and selectivity. Various gas mixtures have been investigated:  $\text{Cl}_2/\text{C}_2\text{F}_4/\text{Ar}$  [7],  $\text{Cl}_2/\text{Ar}$  [6],  $\text{CF}_4/\text{CCl}_4/\text{Ar}$  [8],  $\text{Cl}_2/\text{BCl}_3$  [9]. Influence of etching parameters on the electrical damage evolution has already been studied in the case of chemically assisted bombardment. It seems that both effects including the physical damages and the presence of

chemical residual species on the film surface are not clearly separately studied. However, it is currently assumed that particles bombardment is primarily responsible for the etching whatever the process [10,11]. Moreover, for MEMs applications, the possibility of etching a global structure, such as bottom electrode/ferroelectric film/top electrode, including several materials without having to change the etching gas composition is a very interesting aspect of the pure ion etching.

In this work, we propose a study of pure-Ar ion beam etching on ferroelectric PZT thin films. The electrical property evolution has been systematically evaluated as a function of discharge parameters.

## II. EXPERIMENTAL PROCEDURE

$\text{Pb}(\text{Zr}_{0.54}\text{Ti}_{0.46})\text{O}_3$  thin films were deposited on Pt/Ti/SiO<sub>2</sub>/Si substrates by rf magnetron sputtering with a thickness in the range of 0.9  $\mu\text{m}$  to 1.2  $\mu\text{m}$ . The sputtering conditions are given elsewhere [12]. The PZT films were annealed at 625°C for 30 min to form the PZT perovskite phase.

Ion beam etching (IBE) of PZT was investigated by using Veeco Microetch 3". This system, described elsewhere, was equipped with a Kaufman type source.

The several films were coated with conventional photoresist (Microposit S1813 from Shipley) that was patterned by exposure in a mask aligner. The surface microstructure of unetched and etched PZT was characterized by Atomic Force Microscopy (AFM). Images in the contact mode AFM were carried out using a Park Scientific Instruments Autoprobe CP.

Pt top electrodes were sputtered through a shadow mask on etched PZT to determined electrical property evolution. They were then compared to the unetched samples to evaluate the extent of IBE effect. Capacity,  $\tan\delta$ , and  $C(V)$  were performed using an impedance analyser HP4192A at a frequency of 10kHz and an alternative voltage  $V_{ac}=100$  mV. The ferroelectric loops  $P(E)$  were measured using a standardized Radiant RT6000 system. Measurements were made before and after a top electrode annealing contact at 500°C.

## III. RESULTS AND DISCUSSION

We have shown elsewhere [13] that to achieve an interesting selectivity ratio with IBE technique, it is quite evident that it is desirable to have a current density as low as possible for a given acceleration voltage. For example, we can reach a selectivity of PZT to Ti equal to 2.2 for an acceleration voltage of 600 V and a density of 0.4 mA/cm<sup>2</sup>. By another way, the maximum PZT etch rate of 60 nm/min has been obtained at 1000 V and 1 mA/cm<sup>2</sup>; however, the best selectivity is not achieved with these parameters. So, to find a good compromise between etch rate and selectivity, it seems that the best etching conditions are a current density as low as possible and also a high acceleration voltage.

### a) Surface morphology

The roughness, for different etching conditions, is characterized by the  $r_{ms}$  ( $r_{ms}$  is defined as the root mean square). The results are summarized in Table 1.

	Global roughness (Å)
Unetched PZT	60
Etched PZT (600V , 0.7mA/cm <sup>2</sup> )	229
Etched PZT (1000V , 0.7mA/cm <sup>2</sup> )	413
Etched PZT (800V , 0.5mA/cm <sup>2</sup> )	192
Etched PZT (800V , 1mA/cm <sup>2</sup> )	392

Table 1. Etching influence on PZT roughness

We observe an increase of roughness after etching, with current density and acceleration voltage and also a preferential etch at the grain boundaries. This behavior is probably the result of two combined phenomena. A composition variation between the grain and the boundary and/or a lateral etching inducing a boundaries widening could add to the etching process. It is well known in etch technology that the ion reflections from the feature sidewalls generates a so-called trenching phenomenon.

Figure 1 presents a cross-section view of etched PZT: it allows to compare unetched/etched PZT surface and to observe the etching profile. Moreover, we can see that a high degree of anisotropy is reached under our etching conditions.

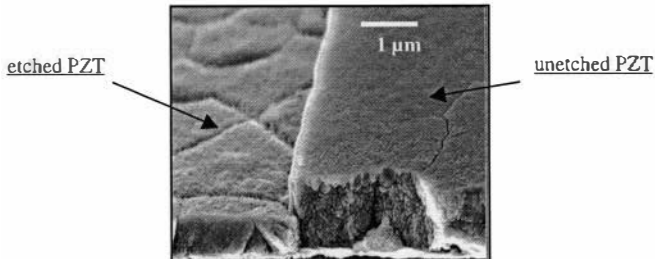


Fig. 1. SEM cross-section view of etch profile at 800V, 0.5mA/cm<sup>2</sup>

### b) Dielectric properties

Electrical properties of unetched and etched PZT films have been compared. After etching in various conditions (by varying the acceleration voltage and the current density), the same final thickness of approximately 0.5μm was obtained for all the samples.

As shown in Figure 2a and 2b, the permittivity  $\epsilon_r$  decreases largely after etching process.  $\epsilon_r$  is more damaged at high current density and at low acceleration voltage. For example, the permittivity value can be reduced from 830 to 520 with a current density and an acceleration

voltage fixed at 0.7mA/cm<sup>2</sup> and 800V. Approximately 10% of this reduction are due to the thickness decreasing. Permittivity measurement were performed with no direct voltage.

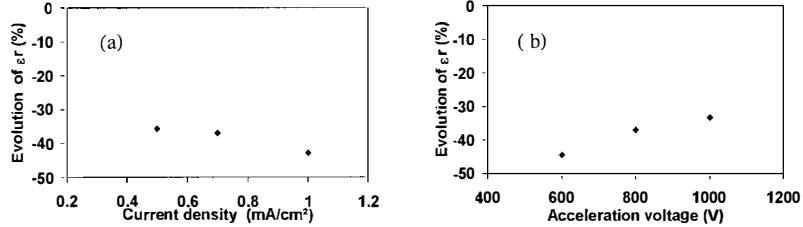


Fig. 2.  $\epsilon_r$  evolution as a function of: a) current density (acceleration voltage = 800V) and b) acceleration voltage (current density = 0.7 mA/cm<sup>2</sup>)

For a same current density, particles of high energy produce less defects. This result shows clearly that more than atoms energy bombarding the film surface it is the increase of atoms density that instigates a stronger permittivity lowering. The  $\epsilon_r$  reduction could be explained by the presence of roughness, amorphized material, charged or neutral defects on the film surface and at the grain boundaries. This damage layer, present in surface, can be considered to have a lower permittivity than ferroelectric PZT and this can induce a smaller dielectric constant for the global structure.

To describe the surface damage layer, we can divided it in two zones. A first layer (layer 1) would consist more especially on an amorphised material, lattice disorder, atom implantation. A second layer (layer 2), includes the same defects at which we have to add the roughness. We can consider that these two layers are not ferroelectric (figure 3).

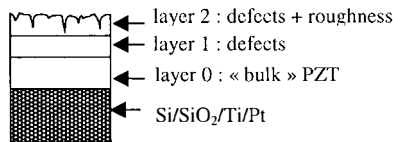


Fig. 3. Schematic cross-section view of etched PZT thin film

When we consider the permittivity evolution as a function of the acceleration voltage, it appears that  $\epsilon_r$  is more reduced at low acceleration voltage, whereas the surface roughness increases with increasing acceleration voltage. So, the roughness seems not to be the predominant factor in the permittivity decreasing and the layer 1 appears to be the main element responsible for the observed evolution. We suggest several hypotheses that could occur at low acceleration voltage:

- The layer 1 permittivity is lower
- The layer 1 thickness is higher

— The layer 1 induces a more important pinning at the interface with the layer 0: higher is the layer 1 thickness, lower is the layer 0 one, and in this case, the influence of the defects present in layer 1 is more and more strong. The  $180^\circ$  domain wall motion is considered to be partly responsible for the permittivity. It was estimated that about 25% to 50% of the dielectric response at room temperature were due to extrinsic source [14]. Therefore, the permittivity decrease could be linked to the domain wall pinning.

Figure 4 shows the permittivity evolution according to the electrical field for various acceleration voltage (a) and various current density (b). These curves allow to distinguish the intrinsic contribution, obtained at saturation field, and the extrinsic contribution associated to the domain wall motion. As the whole, the intrinsic and especially the extrinsic contribution are lowering after etching.

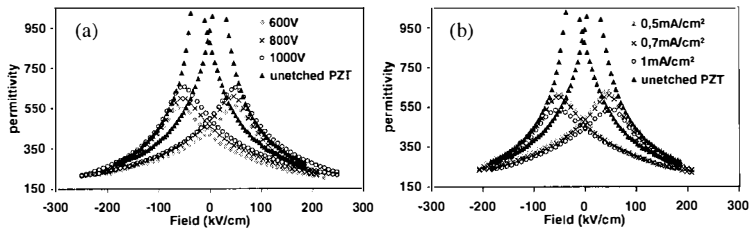


Fig. 4.  $\epsilon_r(E)$  evolution as a function of: a) acceleration voltage (current density =  $0.7 \text{ mA/cm}^2$ ) and b) current density (acceleration voltage =  $800\text{V}$ )

At the coercive field (figure 4a), we note that the extrinsic contribution decreases when the acceleration voltage increases. We can deduce that the domain wall pinning is more strong at low acceleration. However, we observe also a weak increase of the intrinsic contribution (at saturation field) when the acceleration voltage increases. This result could be confirmed by the following hypothesis : for high acceleration voltage, we suggest that the etching is more efficient in comparison with the creation rate of the damage layer (layer 1). As a result, the layer 1 thickness is higher at low acceleration voltage.

Concerning now the permittivity evolution as a function of the current density, we have noted that the decreasing  $\epsilon_r$  with increasing current density coincides with an increasing roughness. However, we have explained previously that the layer 2 roughness can't be the predominant parameter. We think again that the layer 1 is responsible for the results observed, and we formulate the same assumptions as the previous ones. We consider that an increasing current density induces a growing defects density. These many defects can involve the decrease of the layer 1 permittivity : indeed, the lower intrinsic contribution is obtained for the higher current density (figure 4b). Moreover, it is evident that the domain wall pinning is also responsible for the permittivity decrease.

### c) Ferroelectric properties

Maximal and remnant polarization,  $P_m$  and  $P_r$ , evolution follow the same behavior as already observed for the permittivity and hypothesis could have been the same. However, the hysteresis loops measured after etching show a maximum polarization decreasing (between 15

to 25%) while the average remnant polarization is little modified, except for weak acceleration voltage and strong current density. The very weak decrease of the remnant polarization suggests that an important pinning phenomenon occur, preventing the domain back switching. It results from these observations that hysteresis loop is more square. The remarkable part of hysteresis loop after etching film and top electrode annealing (c.a.) is the large increase of the average coercive field  $E_a$ .  $E_a$  is defined as  $E_a = (|E_c^+| + |E_c^-|)/2$ . We can see for example on figure 5 the P(E) curve obtained for PZT etched at 800 V, and 0.7 mA/cm<sup>2</sup>.

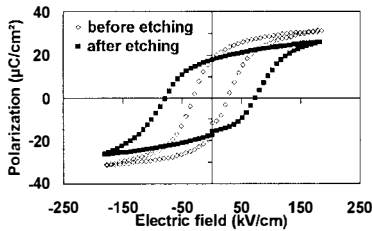


Fig. 5. P(E) hysteresis loop of as-deposited PZT and etched PZT (800V, 0.7mA/Cm<sup>2</sup>) after contact annealing (c.a.)

Similar loops widening, with various magnitudes, were observed for all etched samples. The magnitude of  $E_a$  was measured, as a function of discharge parameters such as current density and voltage acceleration. When acceleration voltage and current density increase, the average coercive field follows an evolution similar to the roughness ones. We could suggest that the damage zone at the film surface is directly responsible for the  $E_a$  increase. The internal field remains very small and we can conclude that the charged defects are present in a weak quantity.

When we compare now the hysteresis loop of etched thin films, before and after top electrode contact annealing, we observe a very interesting damage (Figure 6).

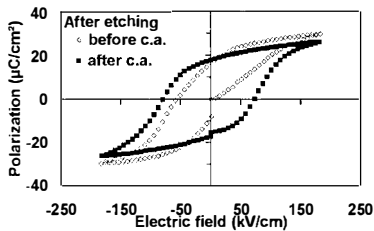


Fig.6. P(E) hysteresis loop of etched PZT (800V, 0.7mA/cm<sup>2</sup>), before and after c.a.

Before contact annealing, an internal electric field was observed for etched as well as unetched PZT. However, this internal field achieves higher values (ranging from -17 to -

23kV/cm) for etched PZT, whatever the etching parameters. The appearance of  $E_i$  is currently assumed to be due to charged defects located at the PZT/Pt interface, or to the presence of a mechanical stress gradient [20]. The presence of the charged defects can be attributed to the deposit of the top-electrode as previously explained, and only the etching process can justify the difference observed in internal field measurement. However, we don't explain the  $E_i$  increase, all the more so since the particles bombarding the surface are atoms. We can suggest that the internal field make easier the switching domain when we apply an electrical field in the same direction. That could justify the weak value for  $E_c^+$  in comparison with  $|E_c^-|$ . However,  $|E_c^-|$  is higher than the result measured for unetched film. After contact annealing, the internal field is partially suppressed and the switching is as difficult in the two directions; then, we have approximately the same value for  $E_c^+$  and  $|E_c^-|$ .  $|E_c^-|$  was increased after contact annealing while generally, for an unetched PZT film,  $|E_c^-|$  remains unchanged before and after c.a. This difference between  $|E_c^-|$  before and after c.a. indicates that the annealing is responsible for a part of the  $E_a$  increasing; during annealing, it's possible that defects induced by atoms bombardment are moving or changing, that could justify an increase of pinning phenomenon. Indeed, by preventing the domain wall motion, a higher electrical field is necessary to allow the domain switching. A 500°C annealing is not able to modify fundamentally layers 1 and 2 (figure 3). On the other hand, a 500°C annealing causes a cross over the Curie temperature and therefore, we think that a modification of the domains distribution and domains walls motion activate defects, inducing pinning.

We have tried to find a post-etching treatment that will be able to enhance the electrical properties after etching. Thermal treatments are often used in this case. A temperature of 550°C is considered as a typical temperature to recover dry etching damage [16].

We propose two types of heat treatment. The first is simply a heat treatment used to crystallize film after the deposit, i.e. an annealing at 625°C for 30min (CA). The second solution that we have tested is a rapid thermal annealing at 700°C during 5s (RTA). In both cases, it concerns heat treatments adapted to the PZT films crystallization. By these means we hope to be able to decrease the defects generated by etching. We noted with these two processes a certain recovery on the permittivity value of 30% by technique RTA and 8% by the technique CA, whereas a profit of 11 à 15% could be obtained on the average coercive field by CA as well as by RTA. Figure 7 shows a comparison of the ferroelectric loops of PZT etched film at 800V and 1mA/cm<sup>2</sup>, and after a heat treatment RTA at 700°C. A sensitive reduction of the pinning seems to be obtained.

We have also supposed that the defects induced during etching could be responsible for oxygen vacancies in the film, particularly if one of the elements PbO, TiO<sub>2</sub> or ZrO<sub>2</sub> is preferentially etched. So, we have decided to perform annealing with oxygen atmosphere. No real improvement of the electrical properties has been observed at 625°C.



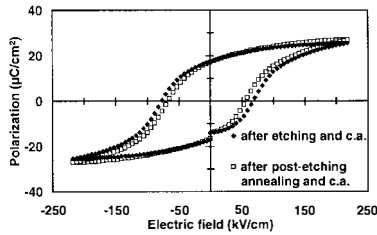


Fig.7. P(E) hysteresis loop of etched PZT (800V, 1mA/cm<sup>2</sup>), before and after post-etching treatment (RTA 700°C-5s), in both cases after c.a.

#### IV. CONCLUSION

In this work, we have presented results concerning the Ar-ion beam etching of PZT thin films. A good compromise between etch rate and selectivity can be achieved working at high acceleration voltage and low current density.

We have shown that the maskless PZT etching generates a large number of damages in terms of surface morphology and electrical properties. Globally, the PZT roughness is largely higher after etching, whatever the etching parameters, and more especially, it increases more and more with increasing current density and acceleration voltage. We have also observed a widening of the grain boundaries; the grain boundaries are preferentially.

When we have compared the electrical results after contact annealing, before and after etching, we have obtained the following evolution: the permittivity is particularly reduced, the maximum polarization decreases whereas the remnant polarization is only little modified, the average coercive field increases and finally the internal field remains practically unchanged. We have proposed various hypotheses to explain these phenomena. At first, the thickness lessening is of course responsible for a part of the evolution observed. We have also considered that the global PZT film can be divided in several layers: a first, corresponding to an amorphized zone with implantation and lattice disorder, a second, including the same defects as well as the surface roughness, and finally, a PZT layer without damage, excepted a possible domain wall pinning induced by the presence of the previous layers. The comparison of ferroelectric properties after etching, before and after contact annealing, allow to show that the annealing is in part responsible for the pinning phenomenon, probably by defects activation.

Heat treatments were proposed in order to decrease the effects of pinning. The results are not very conclusive; indeed, the recovery of the initial electric properties of the PZT film is only partial.

#### Acknowledgment

Scanning electron microscopy observations have been carried out in CMEBA (Rennes University center for scanning electron microscopy and analysis).

## References

- [1] S. Mancha, *Ferroelectrics*, **135**, 131 (1992)
- [2] T. Kawagughi, H. Adachi, K. Setsune, O. Yamazaki, K. Wasa, *Appl. Opt.*, **23**, 2187, (1984)
- [3] K. Saito, J. H. Choi, T. Fukuda, M. Ohue, *Jpn. J. Appl. Phys.*, **31**, L1260, (1992)
- [4] D.P.Vijay, S.B. Desu, W. Pan, *J. Electrochem. Soc.*, **140**, 2635, (1993)
- [5] W. Pan, S.B. Desu, In K. Yoo, D.P. Vijay, *J. Mater. Res.*, **9**, 2976, (1994)
- [6] S. Yokoyama, Y. Ito, K. Ishihara, K. Hamada, T. Ohnishi, J. Kudo, K. Sakiyama, *Jpn. J. Appl. Phys.*, **34**, 767, (1995)
- [7] C. W. Chung, C. J. Kim, *Jpn. J. Appl. Phys.*, **36**, 2747, (1997)
- [8] J. Baborowski, P. Mural, N. Ledermann, E. Colla, A. Seifert, S. Gentil, N. Setter, *Int. Ferr.*, **31**, 261, (2001)
- [9] N. Ikegami, T. Matsui, J. Kanamori, *Jpn. J. Appl. Phys.*, **35**, 2505, (1996)
- [10] J.J. Van Glabbeek, G.A.C.M. Spierings, M.J.E. Ulenaers, G.J.M. Mans, P.K. Larsen, *J. Mat. Res. Symp. Proc.*, **310**, 127, (1993)
- [11] G. Suchanek, R. Tews, G. Gerlach, *Surf. and Coatings Technol.*, **116-119**, 456, (1999)
- [12] G. Velu, D. Rèmesiens, B. Thierry, *J. Europ. Ceram. Soc.*, **17**, 1749, (1997)
- [13] C. Soyer, E. Cattani, D. Rèmesiens, *J. Appl. Phys.*, to be published
- [14] F. Xu, S. Trolrier-McKinstry, W. Pen, B. Xu, Z.-L. Xie, K.J. Hemker, *J. Appl. Phys.*, **89**, 1336, (2000)
- [15] E. G Lec, J. S. Park, J. K. Lee, J. G. Lee, *Thin Solid Films*, **310**, 327, (1997)
- [16] J.K. Lec, T.-Y. Kim, I. Chung, *Appl. Phys. Lett.*, **75**, 334, (1999)